Selective Loss of Sphingosine 1-Phosphate Signaling with No Obvious Phenotypic Abnormality in Mice Lacking Its G Protein-coupled Receptor, LP$_{B3}$/EDG-3*

Isao Ishii‡§, Beth Friedman‡, Xiaoqin Ye‡, Shuji Kawamura‡, Christine McGiffert¶, James J. A. Contos‡, Marcy A. Kingsbury‡, Guangfa Zhang‡, Joan Heller Brown‡¶‖, and Jerold Chun‡¶‖**

From the ‡Department of Pharmacology, the ¶Neurosciences Program, and the ‖Biomedical Sciences Program, School of Medicine, University of California, San Diego, La Jolla, California 92093-0636

Sphingosine 1-phosphate (S1P) exerts diverse physiological actions by activating its cognate G protein-coupled receptors. Five S1P receptors have been identified in mammals: LP$_{B1}$/EDG-1, LP$_{B2}$/H218/AGR16/EDG-5, LP$_{B3}$/EDG-3, LP$_{B4}$/NRG-1/EDG-8, and LP$_{C1}$/EDG-6. One of these receptors, LP$_{B1}$, has recently been shown to be essential for mouse embryonic development. Here we disrupted the lp_{B3} gene in mice, resulting in the complete absence of lp_{B3} gene, transcript, and LP$_{B3}$ protein. LP$_{B3}$-null mice were viable and fertile and developed normally with no obvious phenotypic abnormality. We prepared mouse embryonic fibroblast (MEF) cells to examine effects of LP$_{B3}$ deletion on S1P-induced signal transduction pathways. Wild-type MEF cells expressed lp_{B1}, lp_{B2}, and lp_{B3} but neither lp_{B4} nor lp_{C1}, and they were highly responsive to S1P in phospholipase C (PLC) activation, adenylyl cyclase inhibition, and Rho activation. Identically prepared LP$_{B3}$-null MEF cells showed significant decreases in PLC activation, slight decreases in adenylyl cyclase inhibition, and no change in Rho activation. Retrovirus-mediated rescue of the LP$_{B3}$ receptor in LP$_{B3}$-null MEF cells restored S1P-dependent PLC activation and adenylyl cyclase inhibition. These results indicate a nonessential role for LP$_{B3}$ in normal development of mouse but show nonredundant cellular signaling mediated by a single type of S1P receptor.

Sphingosine 1-phosphate (S1P)[1] is a potent lysophospholipid mediator that exerts diverse biological effects on many types of cells and tissues. S1P is produced from activated platelets and many other cell types and affects fundamental cellular processes including proliferation, differentiation, survival, adhesion, migration, morphogenesis, and cytoskeletal rearrangement (reviewed in Refs. 1–6). S1P has been proposed to act both as an extracellular mediator and an intracellular second messenger. Recent progress in the identification of specific G protein-coupled receptors that can account for the extracellular effects induced by S1P has improved our understanding of the mechanisms of action of this lipid (reviewed in Refs. 1–6).

To date, five cognate G protein-coupled receptors have been identified as mammalian high affinity S1P receptors: LP$_{B1}$/EDG-1, LP$_{B2}$/H218/AGR16/EDG-5, LP$_{B3}$/EDG-3, LP$_{B4}$/NRG-1/EDG-8, and LP$_{C1}$/EDG-6 (reviewed in Refs. 6–8). All S1P receptors belong to a larger lysophospholipid (LP) receptor subfamily, which also includes receptors for lysophosphatidic acid (LPA), a bioactive lipid that is structurally and biologically related to S1P. Each of the LP receptors couples to multiple subsets of heterotrimeric G proteins (including G$_q$, G$_{i/o}$, and G$_{12/13}$) and thus drives different signal transduction pathways. Also, the receptor genes are expressed in spatially and temporally different patterns in mice (9, 10),[2] suggesting specific roles for each receptor *in vivo*. It was reported recently that LP$_{B1}$-null mice are embryonic lethal because of incomplete vascular maturation (11), showing the essential role of LP$_{B1}$ in mouse development. In zebrafish, a single point mutation in an lp_B ortholog, *mil*, led to abnormal heart development (12). To determine *in vivo* functions and roles of the LP$_{B3}$ receptor in mammals, we have disrupted lp_{B3} in mice. Unexpectedly, LP$_{B3}$-null mice were viable and fertile and developed normally with no gross phenotypic abnormality, although selective loss of S1P signal transduction pathways was observed in mouse embryonic fibroblast (MEF) cells. These results continue to clarify physiological functions and roles of the LP$_{B3}$ receptor *in vivo*.

EXPERIMENTAL PROCEDURES

Materials—[α-^{32}P]Deoxy-CTP and *myo*-[2-^{3}H]inositol were purchased from PerkinElmer Life Sciences. S1P and LPA (1-oleoyl-2-hydroxy-*sn*-glycero-3-phosphate) were purchased from Avanti Polar Lipids (Alabaster, AL). GTPγS, platelet-derived growth factor (BB homodimer), and pertussis toxin (PTX) were purchased from Calbiochem. Anti-EDG-3 (LP$_{B3}$) carboxyl and amino terminus monoclonal antibodies were purchased from Exalpha Biological Inc. (Boston, MA). Rhotekin Rho binding domain agarose and PAK-1 p21-binding domain agarose were purchased from Upstate Biotechnology, Inc. (Lake Placid, NY). The pFlox targeting vector (13) and R1 embryonic stem (ES) cells were generous gifts from Dr. Jamey D. Marth (University of California, San Diego). Retrovirus expression vector (LZRSpBMN-linker-IRES-EGFP) and the Phoenix ecotropic retrovirus producer cell lines were kind gifts from Dr. Garry P. Nolan (Stanford University). Trizol and all

[1] The abbreviations used are: S1P, sphingosine 1-phosphate; E14, embryonic day 14; EGFP, enhanced green fluorescent protein; ES, embryonic stem; GTPγS, guanosine 5′-O-(2-thiotriphosphate); kb, kilobase; KO, knockout; LP, lysophospholipid; MEF, mouse embryonic fibroblast; LPA, lysophosphatidic acid; ORF, open reading frame; PCR, polymerase chain reaction; PLC, phospholipase C; PTX, pertussis toxin.

[2] J. J. A. Contos and J. Chun, unpublished observations.

cell culture reagents were purchased from Life Technologies, Inc. Forskolin, 3-isobutyl-1-methylxanthine, and other reagents were purchased from Sigma, unless otherwise noted.

Generation of lp$_{B3}$ Mutant Mice—The isolation of an lp_{B3} λ clone from 129/SvJ mouse genomic DNA library (Stratagene, La Jolla, CA) was described previously (9). The 0.9-kilobase (kb) short arm (an *Apa*I/*Afl*II fragment upstream of the open reading frame (ORF)), the 2.3-kb ORF arm (an *Afl*II/*Afl*II fragment including the entire ORF) and the 2.8-kb long arm (a *Bgl*II/*Xho*I fragment downstream of the ORF) were cloned successively into the pFlox vector, producing the lp_{B3} targeting vector used in this study. The *Not*I-linearized targeting construct was electroporated into R1 ES cells. The targeting was completed by homologous recombination under G418 (200 μg/ml)-positive selection and Cre recombinase-mediated deletion between *loxP* sites under gancyclovir (0.5 μM)-negative selection, which produced both type I (knockout (KO))- and type II-hemizygous cells. The correct integration was confirmed by Southern blot analysis using probes both inside (probe B) and outside (probe A) of the recombination site. A single type I ES clone was injected into C57BL/6N blastocysts to produce chimeric male mice, which were crossed with C57BL/6N females to obtain *agouti* lp_{B3}-heterozygous pups. All mice analyzed were obtained from intercrosses between their progenies and C57BL/6N females. Histological analyses were done on the progenies on a purer C57BL/6N background (backcrossed 3–5 generations). Mice were housed in an air-conditioned room kept on a 12-h dark/light cycle and fed standard dry rodent food pellets *ad libitum*. All animal protocols used in this study have been approved by the Animal Subjects Committee at the University of California, San Diego, and conform to National Institutes of Health guidelines and public laws.

lp_{B3} genotyping was done by Southern analysis and polymerase chain reaction (PCR) using tail genomic DNA as a template and the three primers: primer 1 (5′-CACACAAGCAGACCTCCAGA-3′), primer 2 (5′-TGGTGTGCGGCTGTCTAGTCAA-3′), and primer 3 (5′-ATCGATACCGTCGATCGACCT-3′). The PCR condition was 35 cycles of 94 °C for 30 s, 56 °C for 1 min, and 72 °C for 1 min.

Northern Blot Analysis—Mouse tissue was quickly removed and homogenized in the Trizol reagent with the Tissue Tearor (Biospec Products, Bartlesville, OK). Total RNA was isolated following Life Technologies' instructions, and 20 μg of each RNA was analyzed as described previously (14). Specific probes used were the ORF sequences for mouse lp_{B1-B4} and lp_{C1} cDNA. lp_{B1-B3} were isolated as described previously (9). lp_{B4}[3] (GenBank™ accession number AF327535) and lp_{C1} cDNA[2] were isolated from 129/SvJ mouse genomic DNA library and Swiss/Webster-NIH cDNA library (CLONTECH), respectively. The blot was also hybridized with a mouse housekeeping glyceraldehyde-3-phosphate dehydrogenase gene as a loading control.

Western Blot Analysis—Mouse tissue was quickly removed and homogenized by 100 strokes of the Tissue Grind Pestle (Kontes Glass Company, Vineland, NJ) in buffer (Tris-Cl (pH 7.6), 150 mM NaCl, 5 mM EDTA, 1 mM EGTA, 1 mM dithiothreitol, 1 mM phenylmethylsulfonyl fluoride, 1 × Protease Inhibitor Cocktail Set I (Calbiochem)). The homogenate was centrifuged at 1,000 × g for 5 min at 4 °C, and the supernatant was further centrifuged at 15,000 × g for 20 min at 4 °C to precipitate crude membrane fraction. This fraction was solubilized in the sample buffer (60 mM Tris-Cl (pH 6.8), 6% (v/v) glycerol, 1.7% SDS, 100 mM dithiothreitol), sonicated for 5 min in the water bath-type ultrasonicator (FS3 Ultrasonic Cleaning System; Fisher), separated on a 10% SDS-polyacrylamide gel, and transferred to the Protran nitrocellulose membranes (Schleicher & Schuell). Because heat denaturation in the SDS-containing sample buffer before gel fractionation diminished the bands specific to the wild-type samples, the loaded sample was sonicated but not heated for complete denaturation. The LP$_{B3}$ protein was detected with anti-LP$_{B3}$ antibodies directed against carboxyl or amino terminus using the Vectastain Elite ABC kit (Vector Laboratories, Burlingame, CA) and ECL Plus detection system (Amersham Pharmacia Biotech).

Histological Analysis—lp_{B3}-heterozygous males and females were bred to obtain all three genotypes, wild-type ($lp_{B3}^{+/+}$), heterozygous ($lp_{B3}^{+/-}$), and knockout ($lp_{B3}^{-/-}$), within the litters, and these littermates were analyzed comparatively at three developmental stages (10 days, 4 weeks, and 8 weeks). The mice were anesthetized with Nembutal sodium solution (0.75 mg/g body weight) (Abbott). Anesthetized mice were perfused through the heart with 0.9% NaCl, followed by 4% paraformaldehyde in phosphate-buffered saline. Each tissue was dissected out, postfixed overnight in 4% paraformaldehyde in phosphate-buffered saline at 4 °C, and processed for paraffin embedding. Parasag-

ittal sections (5 μm) were cut, processed, and stained with hematoxylin and eosin according to standard protocols.

In Situ Hybridization—lp_{B3}-heterozygous male and female were bred to obtain both wild-type and knockout littermates. Pregnant female was sacrificed by cervical dislocation, and embryonic day 14 (E14) embryos were removed, rapidly frozen in the Tissue-Teck optimal cutting temperature compound (Miles, Elkhart, IN), and stored at −80 °C until sectioned. Digoxigenin-labeled riboprobes were transcribed in the sense and antisense orientations from linearized plasmids containing the entire mouse lp_{B3} ORF. Parasagittal cryostat sections (20 μm) were cut, and adjacent sections were hybridized with either sense or antisense riboprobes and processed as described previously (15, 16).

Preparation of MEF Cells—MEF cells were prepared from E14 embryos generated by the wild-type or knockout intercrosses. Briefly, the heads and internal viscera were removed, and the carcasses were finely minced with scissors and digested by incubation in 0.05% trypsin, 0.53 mM EDTA solution for 30 min at 37 °C with gentle agitation. Trypsin was inactivated by adding the culture medium (Dulbecco's modified Eagle's medium supplemented with 10% heat-inactivated fetal bovine serum (Hyclone, Logan, UT) and antibiotics), and the cells were filtrated through a 70-μm cell strainer (Becton Dickinson Labware, Franklin Lakes, NJ) and seeded onto tissue culture dishes. MEF cells were maintained as a monolayer culture on tissue culture dishes in the culture medium, and cells from the second to third passages were used.

Construction of Retrovirus Vectors and Production of Retrovirus Supernatants—The entire ORF of each receptor was cloned into the pFLAG-CMV-1 mammalian expression vector (Eastman Kodak Co.) for introducing preprotrypsin leader/FLAG tag sequences into an extracellular amino terminus of each receptor. This procedure enabled higher expression levels of the receptors in the plasma membrane and immunochemical detection of the receptors (data not shown; see Ref. 14). Next, all coding sequences were cloned into the retrovirus vector, LZR-SpBMN-linker-IRES-EGFP, and inserts of the construct were confirmed by sequencing. The internal ribosome entry site sequence in the retroviral vector permitted concomitant expression of the receptor gene and enhanced green fluorescent protein (EGFP) gene from a single transcript driven by a 5′-long terminal repeat promoter, allowing identification of infected (living and fixed) cells by fluorescence microscopy. High titer, helper-free retrovirus supernatant was prepared using the Phoenix producer cell lines as described (14).

Retrovirus Infection—Viral supernatant supplemented with 5 μg/ml hexadimethrine bromide was added to MEF cells on multiwell dishes, and the dishes were centrifuged (700 × g) at 32 °C for 1 h (14). The cells were cultured for 24 h, incubated in serum-free medium for another 24 h, and then used for each experiment. Receptor gene and protein expression were confirmed by Northern blot analysis and immunostaining using anti-FLAG antibody, respectively (data not shown; refer to Ref. 14). By counting the numbers of cells with EGFP fluorescence (infected cell numbers) and cells with 4′,6-diamidino-2-phenylindole fluorescence (total cell numbers) on fixed samples, an effective infection in MEF cells of >50% of total cells was confirmed. Infection was routinely confirmed by EGFP fluorescence from the living cells (14).

Phospholipase C (PLC) Assay—MEF cells on 12-well dishes were prelabeled with [³H]inositol (2 μCi/well) in inositol-free, serum-free Dulbecco's modified Eagle's medium for 24 h. The cells were then incubated for 30 min in Hepes/Tyrode's/bovine serum albumin buffer (17) containing 10 mM LiCl and stimulated with S1P or LPA. After a 20-min incubation, the reaction was terminated by aspirating the buffer and adding 500 μl of ice-cold 0.4 M HClO$_4$. Radioactivity in the inositol phosphate (IP$_1$ + IP$_2$ + IP$_3$) fractions of the samples was examined as described previously (14, 17). The activity was expressed as the -fold induction above a basal level.

Measurement of Intracellular cAMP Contents—cAMP contents were measured with the cAMP enzyme immunoassay system (Amersham Pharmacia Biotech) following the manufacturer's instructions. MEF cells on 24-well dishes were preincubated in Hepes/Tyrode's/bovine serum albumin buffer containing 0.5 mM 3-isobutyl-1-methylxanthine for 20 min. The cells were then stimulated for 20 min with or without 1 μM forskolin in the presence or absence of various concentrations of S1P. The reaction was terminated by aspirating the buffer and adding 500 μl of the lysis reagent 1B (as per Amersham Pharmacia Biotech instructions). After a 20-min extraction, 100 μl of the supernatant was collected for cAMP determination. The activity was expressed as a percentage of forskolin (1 μM)-induced cAMP accumulation.

Determination of Rho and Rac Activation—MEF cells on 10-cm dishes were incubated for 10 min in Hepes/Tyrode's/bovine serum albumin buffer and then stimulated with S1P. The reaction was terminated by washing the cells with ice-cold phosphate-buffered saline and
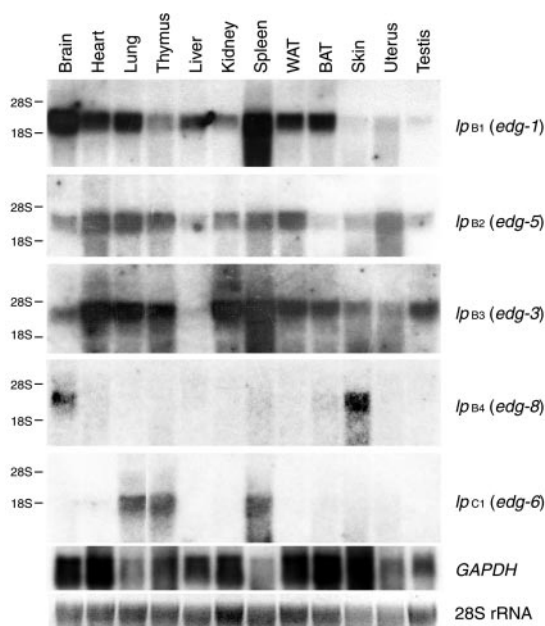
FIG. 1. **Expression patterns of the five S1P receptor genes in 8-week-old C57BL/6N (background strain) mouse tissues.** Total RNA (20 μg each lane) of various tissues from female mice (except testis) was examined by high stringency Northern blot analysis using specific probes to mouse lp_{B1-B4} and lp_{C1}. *WAT* and *BAT*, white adipose tissue and brown adipose tissue, respectively. As loading controls, ribosomal 28 S RNA was stained with ethidium bromide, and the blot was probed with glyceraldehyde-3-phosphate dehydrogenase (*GAPDH*). *28S* and *18S* indicate the positions of mouse ribosomal RNA, which are 4.7 and 1.9 kb, respectively.

lysing in 600 μl of the lysis buffer (50 mM Tris-Cl (pH 7.6), 1% (w/v) Triton X-100, 500 mM NaCl, 10 mM MgCl$_2$, 10 μg/ml each of leupeptin and aprotinin, and 1 mM phenylmethylsulfonyl fluoride). Cell lysates were centrifuged at 13,000 $\times$ g at 4 °C for 10 min, and equal volumes of supernatants were incubated with rhotekin Rho binding domain (for Rho activity) or PAK-1 p21-binding domain (for Rac activity) agarose beads at 4 °C for 45 min. The beads were washed four times with the washing buffer (0.1% (w/v) Triton X-100, 150 mM NaCl, 10 mM MgCl$_2$, 10 μg/ml each of leupeptin and aprotinin, and 0.1 mM phenylmethylsulfonyl fluoride). Bead-bound, GTP-bound active forms of Rho and Rac proteins were specifically detected by Western blot analysis using anti-Rho A (Santa Cruz Biotechnology, Inc., Santa Cruz, CA) and anti-Rac 1 (Transduction Laboratories, Lexington, KY) monoclonal antibodies. Rho proteins in 5% and Rac proteins in 1% of the cell lysates were also detected as references.

Data Representation—Data are the means ± S.E. of triplicate samples from a single experiment that was representative of 2–3 experiments that gave similar results. Statistical analysis was done by Student's t test or χ^2 test (only in Table I), and the difference at $p < 0.05$ was considered to be statistically significant.

RESULTS

Expression of lp_{B3} in Mice—To examine wild-type expression patterns of each of the five S1P receptor genes in C57BL/6N mice, total RNA from 8-week-old female tissues (except male testis) was analyzed by Northern blot using mouse ORF probes (Fig. 1). The lp_{B1-B3} expression pattern in brain, heart, lung, thymus, liver, kidney, and spleen, was consistent with our previous results obtained from analyses of adult BALB/c mice (9). Also, we analyzed the expression of these genes in adipose tissues (both white and brown), back skin, and sex organs (uterus and testis). Each lp_{B1-B3} was expressed to various degrees in all tissues examined with the exception of liver, where no detectable lp_{B3} expression was found. In contrast, the expression of lp_{B4} and lp_{C1} was more specific. lp_{B4} was expressed at detectable levels only in brain and skin among the tissues we analyzed, while lp_{C1} was expressed only in lung, thymus, and spleen.
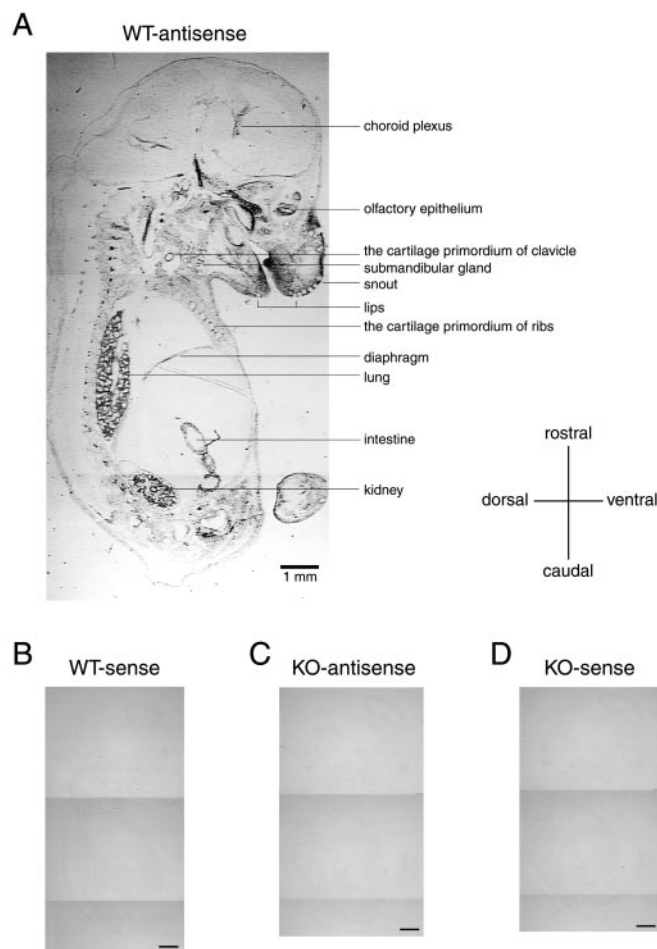

FIG. 2. **lp_{B3} in situ hybridization of wild-type and LP$_{B3}$-null E14 embryos.** Shown is the *in situ* hybridization of parasagittal sections from E14 wild-type and knockout littermates with digoxigenin-labeled antisense and sense lp_{B3} riboprobes. Antisense probe detected lp_{B3} expression in wild-type (*WT*) mouse (*A*) but not in knockout (*KO*) mouse (*C*). Negative control sense probe did not detect any specific labeling in both wild-type (*B*) and knockout (*D*) mouse. *Scale bars*, 1 mm.

To determine lp_{B3} expression during embryonic development, we used *in situ* hybridization on E14 embryos (Fig. 2). Antisense probes detected high lp_{B3} expression in lung, kidney, intestine, diaphragm, submandibular gland, olfactory epithelium, choroid plexus, the cartilage primordium of ribs and clavicle, and the presumptive cartilaginous regions of lips (lower and upper) and snout regions but, as we found with adults, not in liver (Fig. 2*A*). The corresponding sense strand probe was used as a negative control and did not show any specific labeling (Fig. 2*B*). The different levels of lp_{B3} expression found when comparing the Northern blot *versus* the *in situ* hybridization results might reflect changing expression levels during mouse development; note lp_{B3} expression level in embryonic heart (low) *versus* expression level in 8-week-old adult heart (high).

Generation of LP$_{B3}$-null Mice—The genomic structure of lp_{B3} consists of two exons, with the entire ORF encoded in the second exon (Fig. 3*A* and data not shown). The entire ORF was deleted in R1 ES cells using the Cre-*loxP* system (13), which allows for the removal of selectable enzyme marker genes and their associated constitutive promotors (this is the constitutive "type I" deletion) (Fig. 3*A*). In a similar manner, we also produced ES cells with the conditional "type II" deletion, in which the ORF is flanked by *loxP* sites (Fig. 3*A*). Only the type I ES cells (Fig. 3*B*, *left*) were injected into blastocysts, and a series of
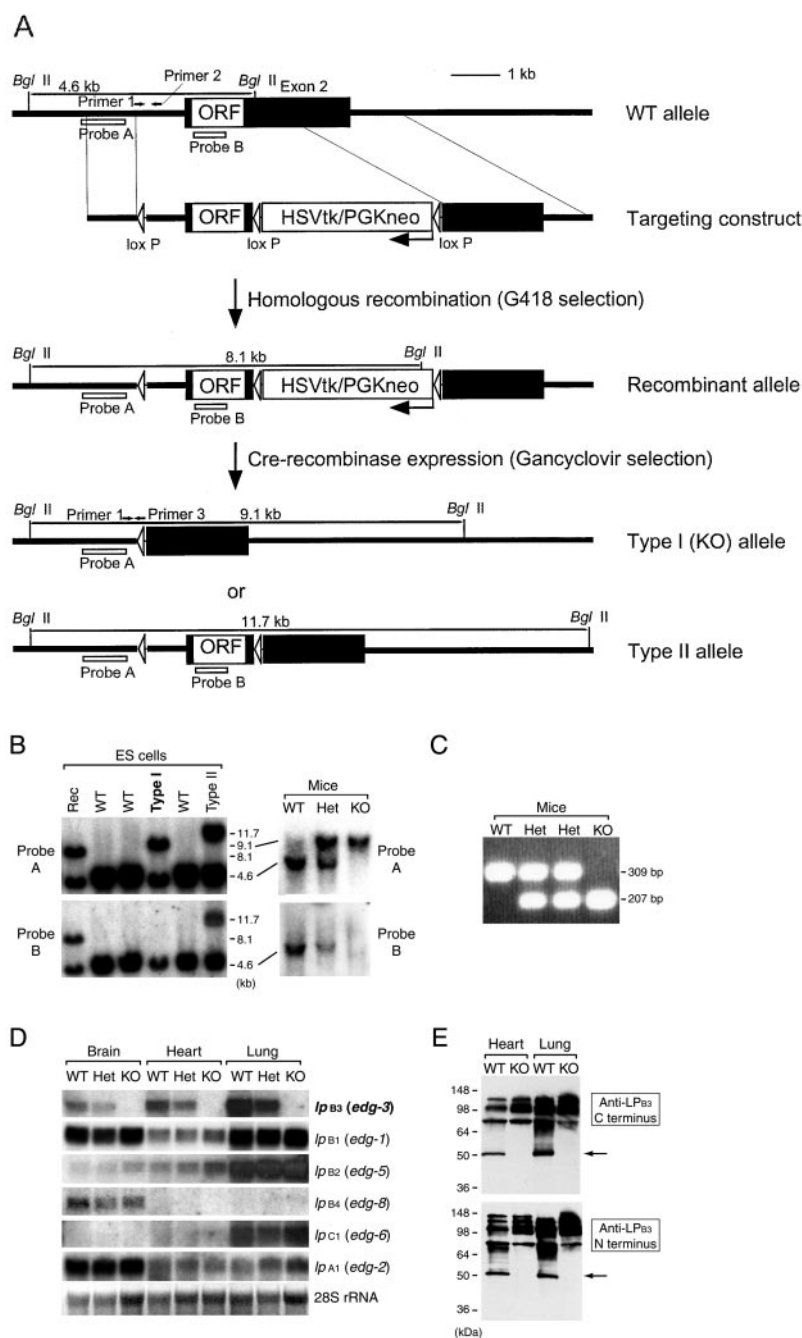
FIG. 3. **Generation of the LP$_{B3}$-null mice.** *A*, lp_{B3} gene targeting using the Cre-*loxP* system. Structures of wild-type allele, targeting construct, recombinant (*Rec*) allele, type I (knockout) allele, and type II allele, are shown. *WT*, wild-type; *KO*, knockout. Southern probes and sizes of the restriction enzyme fragments detected with the probes are indicated. Approximate positions of PCR primers used for genotyping are also shown. *B*, Southern blot analysis of *Bgl*II-digested genomic DNA from both properly targeted R1 ES cell clones (recombinant, type I, and type II) and mouse tails prepared from pups generated by crossing heterozygotes (*Het*). *C*, PCR genotyping of each mouse tail DNA to detect the wild-type, heterozygous, and knockout alleles (PCR product sizes: 309 and 207 base pairs, respectively). *D*, Northern blot analysis of RNA from brain, heart, and lung isolated from adult wild-type, heterozygous, and knockout male littermates. The probes used are indicated to the *right*. Ribosomal 28 S RNA was stained with ethidium bromide as a loading control. *E*, Western blot analysis of crude membrane fraction samples from heart and lung tissues of wild-type and knockout mice. Both anti-LP$_{B3}$ carboxyl and amino terminus (C and N terminus, respectively) monoclonal antibodies detect a ~50-kDa protein specific to the wild-type samples.

mice with mutated alleles ($lp_{B3}{}^{+/-}$ or $lp_{B3}{}^{-/-}$) was established (Fig. 3, *B* (*right*) and *C*). The complete absence of lp_{B3} transcripts in the knockout mice was confirmed both by Northern blot analysis on adult tissues in which lp_{B3} is normally expressed: brain, heart, and lung (Fig. 3*D*) and *in situ* hybridization on E14 embryos (Fig. 2*C*). There was moderate lp_{B3} expression in heterozygous tissues (Fig. 3*D*). In most of those tissues, the other S1P receptor genes (lp_{B1}, lp_{B2}, lp_{B4}, and lp_{C1}) and an LPA receptor gene (lp_{A1}) were also expressed. LP$_{B3}$ deficiency appeared to lead to compensatory increases in lp_{B2} expression levels in brain and heart but not in lung, uterus, or testis, whereas no compensatory increases were found in the other gene expression levels (Fig. 3*D* and data not shown). LP$_{B2}$ protein expression could not be addressed in those tissues because specific anti-LP$_{B2}$ antibodies to detect mouse LP$_{B2}$ protein are not available. The complete absence of LP$_{B3}$ protein in the knockout mice was confirmed by Western blot analysis

on the crude membrane fractions isolated from heart and lung (Fig. 3*E*). Both anti-LP$_{B3}$ antibodies (directed against either the carboxyl or amino terminus) detected a ~50-kDa protein in the wild-type but not in knockout mouse tissues. The molecular weight of the LP$_{B3}$ protein estimated from mouse lp_{B3} sequences is 42.3 kDa. The difference between our results and the estimated molecular weights may result from the sample not being heated for denaturation before gel fractionation (see "Experimental Procedures") and might explain the slower migration of the receptor protein. In addition, the size difference may reflect possible posttranslational modification of the receptor protein such as extracellular amino terminus glycosylation and intracellular carboxyl terminus palmitoylation (9).

No Gross Phenotypic Abnormality in LP$_{B3}$-null Mice—LP$_{B3}$-null mice were generally obtained at the expected Mendelian frequency and without sexual bias (χ^2 test; Table I). Homozygous-null matings produced LP$_{B3}$-null pups, although the av-

TABLE I
Inheritance of the Ip$_{B3}$ mutant allele

Total litter numbers, average litter sizes (means ± S.D.), and numbers of genotyped offspring from the indicated crosses are shown. The litter sizes from the homozygous intercrosses were significantly smaller than those from the crosses between heterozygous (Het) males and wild-type (WT) females (*, $p < 0.01$). KO, knockout.

Parental genotypes	Total litter numbers	Average litter sizes	Offspring genotypes at weaning ages (~3 weeks)								
			Males			Females			Both sexes		
Male × Female			WT	Het	KO	WT	Het	KO	WT	Het	KO
Het × WT	18	7.5 ± 2.7	47	29		27	32		74	61	
Het × Het	57	6.5 ± 2.2	60	96	40	38	91	43	98	187	83
Het × KO	24	6.6 ± 1.9		43	33		43	39		86	72
KO × Het	21	6.9 ± 2.4		42	33		30	39		72	72
KO × KO	25	5.6 ± 1.8			63			78			141

(*, bracket spanning Average litter sizes from Het × WT through KO × KO)

erage litter size was modestly but significantly smaller ($p < 0.01$) than the size from the crosses between heterozygous males and wild-type females (5.6 *versus* 7.5 pups per litter). Knockout mice did not differ from the wild-type or heterozygous littermates in overall health, body weight, fertility, or longevity (through at least 18 months). During embryonic stages, the knockout mice were indistinguishable from their wild-type littermates (data now shown). Routine histology that examined tissues from mice of age 10 days, 4 weeks, and 8 weeks (brain, heart, lung, thymus, liver, kidney, spleen, adipose tissues, skin, muscle, stomach, intestine, uterus, and testis) revealed no obvious abnormality (data not shown). Also, routine hematology including erythrocyte, leukocyte, and platelet counts; neutrophil, lymphohocyte, monocyte, and eosinophil proportions; and glucose, cholesterol, and triglyceride serum levels as well as lipase activity failed to detect any abnormalities or differences in the knockout *versus* wild-type mice (data not shown). Despite lp_{B3} expression in adult skin (Fig. 1), the knockout mice were indistinguishable from their wild-type littermates in thickness of epidermal layers and numbers of hair follicles (data not shown).

S1P Receptor Expression in MEF Cells—To determine the contribution of lp_{B3} to S1P signaling, we utilized MEF cells derived from E14 embryos to analyze S1P-induced signal transduction pathways. Wild-type MEF cells expressed lp_{B1}, lp_{B2}, and lp_{B3} but neither lp_{B4} nor lp_{C1} at levels detectable by Northern blot analysis (Fig. 4). As expected, LP$_{B3}$-null MEF cells lacked lp_{B3} expression. LP$_{B3}$ deficiency did not lead to compensatory increases in the expression of other S1P receptor genes in the knockout MEF cells (Fig. 4). In various cell systems, LP$_{B1}$ receptor has been shown to couple only to PTX-sensitive G$_{i/o}$ proteins. In contrast, both LP$_{B2}$ and LP$_{B3}$ receptor have been shown to couple to G$_q$, G$_{i/o}$, and G$_{12/13}$ proteins (reviewed in Refs. 6 and 8). Therefore, we analyzed S1P induction of downstream events activated by these types of G proteins including PLC activation, inhibition of adenylyl cyclase activation, and Rho activation.

Significant Decrease in S1P-induced PLC Activation in LP$_{B3}$-null MEF Cells—MEF cells prelabeled with [³H]inositol were stimulated with various concentrations of S1P for 20 min, and the radioactivity in inositol phosphate fractions was measured. S1P activated PLC in the wild-type cells in a concentration-dependent manner, giving a marked stimulation at concentrations between 0.1 and 10 μM (Fig. 5A, *left*). In contrast, S1P treatment led to only modest PLC activation in LP$_{B3}$-null MEF cells, inducing 15–20% of the response achieved in the wild-type cells at concentrations up to 10 μM. MEF cells also express at least two LPA receptor genes, lp_{A1} and lp_{A2},[4] which encode proteins shown to respond to LPA with activation of PLC in various cell systems (14, 18). Wild-type MEF cells were highly
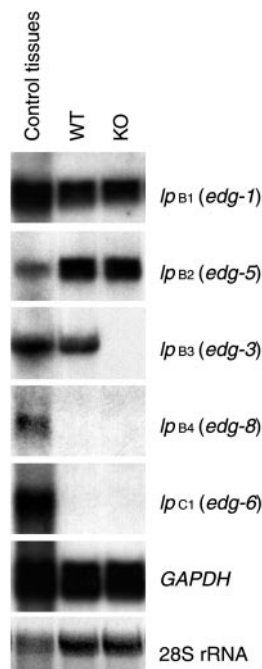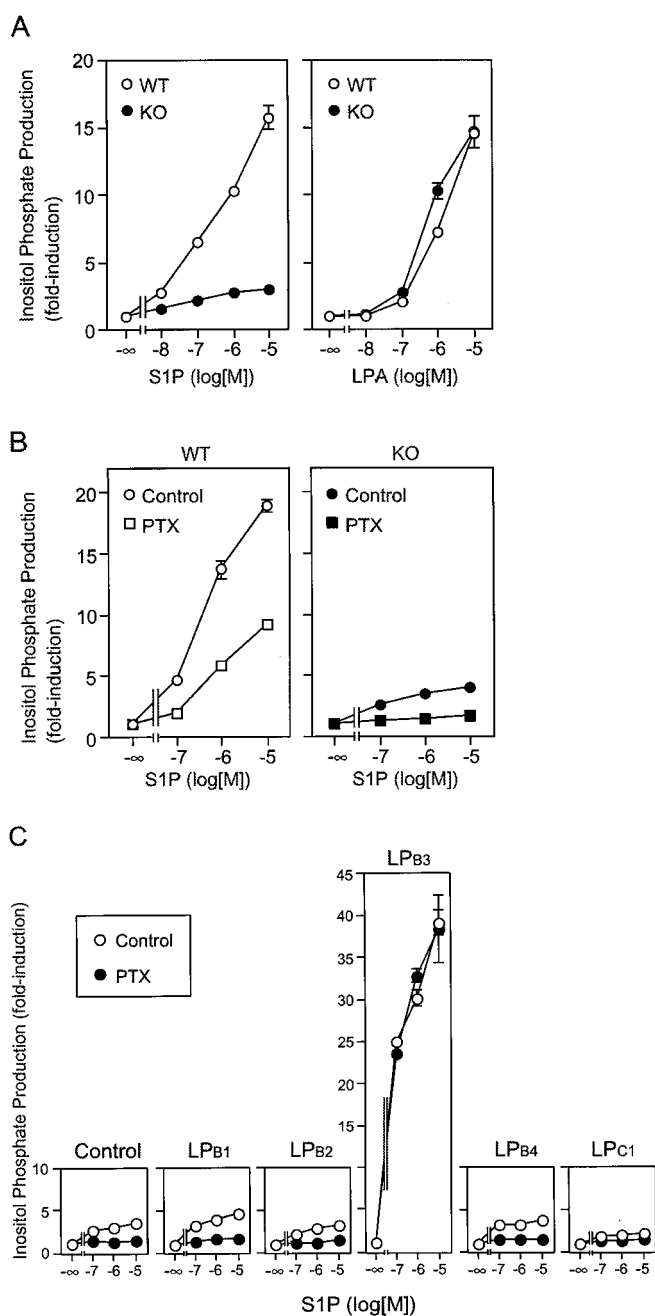

FIG. 4. **Expression of S1P receptor genes in wild-type and LP$_{B3}$-null MEF cells.** MEF cell RNA prepared from wild-type and knockout E14 embryos was analyzed by Northern blot analysis. *WT*, wild-type; *KO*, knockout. The knockout MEF cells lack lp_{B3} expression. Tissue RNA isolated from an adult C57BL/6N female was used as a positive control (heart RNA for lp_{B1-B3}, brain RNA for lp_{B4}, and lung RNA for lp_{C1}). As loading controls, ribosomal 28 S RNA was stained with ethidium bromide, and the blot was probed with glyceraldehyde-3-phosphate dehydrogenase (*GAPDH*).

responsive to LPA, and LPA-induced PLC activation was comparable in the wild-type and knockout cells (Fig. 5A, *right*), demonstrating that lipid receptor coupling to PLC is not generally impaired. S1P-induced PLC activation in the wild-type cells was partially sensitive to PTX pretreatment (Fig. 5B, *left*), suggesting the involvement of both PTX-sensitive and insensitive proteins. In LP$_{B3}$-null MEF cells, however, the residual, small S1P-induced PLC activation was fully inhibited by PTX pretreatment, indicating that it was mediated through a G$_{i/o}$ pathway (Fig. 5B, *right*).
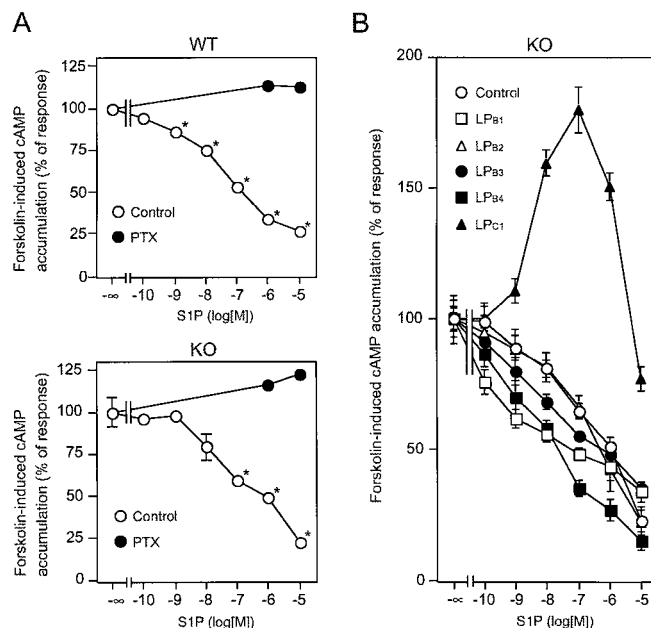
To ascertain whether the decreased responses in the knockout cells were a direct result of the LP$_{B3}$ deficiency as opposed to nonspecific effects secondary to gene targeting or MEF cell preparation, functional LP$_{B3}$ and other S1P receptors were exogenously expressed in the knockout MEF cells using the retrovirus-mediated system (14, 19) (Fig. 5C). Introduction of lp_{B3} into LP$_{B3}$-null MEF cells led to a marked increase (~10-fold increase *versus* cells infected with control virus) in S1P-stimulated PLC activation, which was not inhibited by PTX pretreatment (Fig. 5C). Introduction of lp_{B1} caused a doubling

[4] I. Ishii and J. Chun, unpublished observations.

FIG. 6. **S1P-induced inhibition of forskolin-induced cAMP accumulation in MEF cells.** MEF cells were stimulated with increasing concentrations of S1P for 20 min in the presence of 1 μM forskolin and 0.5 mM 3-isobutyl-1-methylxanthine. Intracellular cAMP content was measured by the enzyme immunoassay. *A*, S1P-induced inhibition of forskolin-induced cAMP accumulation in wild-type and knockout MEF cells. *WT*, wild-type; *KO*, knockout. The inhibitory effect of S1P is significant (*, $p < 0.01$). PTX pretreatment (100 ng/ml, 24 h) completely abolished S1P effects in both cells. *B*, S1P-induced inhibition of forskolin-induced cAMP accumulation in knockout MEF cells infected with each of the S1P receptor-expressing retroviruses. In all panels, forskolin-induced cAMP accumulation was expressed as 100%. Data shown are the means ± S.E. of triplicate samples from representative experiment. S.E. bars are not shown when bars are smaller than the size of the data points.

FIG. 5. **S1P-induced inositol phosphate production in MEF cells.** MEF cells prelabeled with [^{3}H]inositol were stimulated with S1P or LPA for 20 min, and the radioactivity in inositol phosphate fraction of the cell extract was determined. *A*, S1P- and LPA-induced inositol phosphate production in wild-type and knockout MEF cells. *WT*, wild-type; *KO*, knockout. *B*, S1P-induced inositol phosphate production in PTX (100 ng/ml, 24 h)-treated and untreated cells. *C*, S1P-induced inositol phosphate production in the knockout MEF cells infected with each of the S1P receptor-expressing retroviruses. The activity is expressed as -fold induction above control levels. Data shown are the means ± S.E. of triplicate samples from the representative experiment. S.E. bars are not shown when bars are smaller than the size of the data points.

of the S1P response, and this was completely inhibited by PTX pretreatment (Fig. 5*C*). None of the other S1P receptors including LP$_{B2}$ restored the responses to S1P in MEF cells. In contrast, retroviral expression of lp_{B2} in B103 rat neuroblastoma cells resulted in the enhancement of S1P (1 μM)-induced PLC response (6.4-fold induction in infected cells *versus* 4.9-fold induction in control cells), suggesting that LP$_{B2}$ can activate PLC in other cell systems. These results indicate that, at least

in MEF cells, LP$_{B3}$ is the primary receptor involved in PTX-insensitive, S1P-induced PLC activation.

Slight Decrease in S1P-induced cAMP Inhibition in LP$_{B3}$-null MEF Cells—In wild-type MEF cells, S1P did not change the basal cAMP level (data not shown) but greatly inhibited the forskolin (1 μM)-induced cAMP accumulation in a concentration-dependent manner (Fig. 6*A*, *top*). The inhibitory effect was observed at concentrations as low as a 0.1 nM, reaching ~75% inhibition at 10 μM. This effect was completely blocked by PTX pretreatment. In LP$_{B3}$-null MEF cells, S1P still inhibited cAMP accumulation, although the concentration-response curve was slightly right-shifted (Fig. 6*A*, *bottom*). As in the wild-type cells, this inhibition was completely blocked by PTX pretreatment. These findings suggest that the LP$_{B3}$ receptor can mediate G$_{i/o}$-mediated inhibition of cAMP accumulation, but that other receptors provide the major activation of this pathway. To support our findings from receptor overexpression studies, retroviruses were used to express each receptor in LP$_{B3}$-null MEF cells. The expression of lp_{B1}, lp_{B3}, or lp_{B4} shifted the S1P-induced inhibitory curve to lower concentrations (Fig. 6*B*). The expression of lp_{B2} did not cause significant alterations. In contrast, the expression of lp_{C1} led to robust increases in cAMP accumulation at lower concentrations (1–100 nM), which was reversed at higher concentrations. All these results suggest that LP$_{B1}$, LP$_{B3}$, and LP$_{B4}$ induce adenylyl cyclase inhibition while LP$_{C1}$ induces adenylyl cyclase activation in the presence of forskolin. Because endogenous lp_{B4} was not expressed at detectable levels in MEF cells, LP$_{B1}$ may be the primary receptor mediating inhibitory actions of S1P, with LP$_{B3}$ playing a minor role.

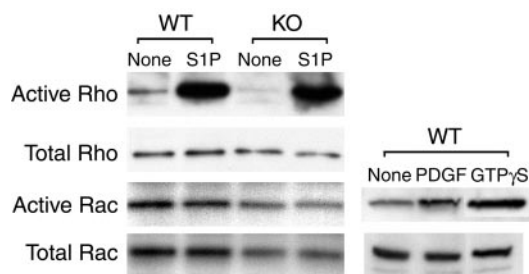*No Significant Difference in S1P-induced Rho Activation in*

FIG. 7. **S1P-induced Rho and Rac activation in MEF cells.** Wild-type (*WT*) and knockout (*KO*) MEF cells were stimulated with 1 μM of S1P for 3 min, and the cell lysate was used for affinity precipitation to pull down activated forms of Rho and Rac. As positive controls for the Rac assay, both wild-type MEF cells were stimulated with 50 ng/ml platelet-derived growth factor (*PDGF*) for 5 min, and wild-type MEF cell lysate was incubated with GTPγS (100 μM) and EDTA (10 mM) for 15 min. Portions of total cell lysate (5 and 1% for Rho and Rac, respectively) were used to determine Rho and Rac levels. Samples were separated on 15% SDS-polyacrylamide gels and analyzed by Western blot analysis using anti-Rho A and anti-Rac 1 antibodies. Data are representative from three independent experiments.

MEF Cells—S1P-induced activation of the small GTPases, Rho and Rac, was assayed in MEF cells (Fig. 7). At 3 min after S1P stimulation of the cells, the "active" GTP-bound forms of Rho and Rac proteins were selectively collected using affinity precipitation with rhotekin Rho binding domain and PAK-1 p21-binding domain beads, respectively (see "Experimental Procedures"). Total Rho and Rac proteins were analyzed as references. S1P activated Rho but not Rac in the wild-type MEF cells. Rac activation was not observed at 1, 3, 5, and 15 min after S1P (1 μM) stimulation (data not shown). However, Rac activation was observed at 5 min after platelet-derived growth factor (50 ng/ml) stimulation or cell lysate *in vitro* incubation (15 min at 30 °C) with GTPγS (100 μM) and EDTA (10 mM) (Fig. 7). Rho activation was not inhibited by PTX pretreatment (data not shown). A similar response was also observed in LP$_{B3}$-null MEF cells (Fig. 7), suggesting that LP$_{B3}$ is not the primary receptor subtype involved in S1P-induced Rho activation in MEF cells.

DISCUSSION

Molecular identification of mammalian S1P receptors (9, 20–24) has furthered our understanding of the versatility of this simple lipid. These receptors belong to the mammalian LP receptor subfamily of G protein-coupled receptors, which includes five S1P receptors and three LPA receptors (LP$_{A1-A3}$) (reviewed in Refs. 4, 6, and 8). The existence of multiple receptors for a single ligand suggests distinct receptor functions *in vivo*, and this view has been supported by the different phenotypes of mice null for a single S1P receptor (11) or LPA receptor (25). Whether LP receptors within S1P or LPA receptor subgroups produce related phenotypes when genetically deleted is uncertain, providing a major rationale for the current study.

A wealth of *in vitro* work has implicated LP$_{B3}$ as essential for S1P-induced cellular responses that include proliferation (26, 27), migration (26, 28, 29), survival (27, 30), and morphogenesis (30, 31). In particular, antisense-mediated down-regulation of LP$_{B1}$ and LP$_{B3}$ signaling in human umbilical vein supported their requirement for endothelial cell assembly to form capillary-like networks preceding angiogenesis (31), as well as for endothelial cell migration (32). Along these lines, genetic deletion of LP$_{B1}$ produced embryonic lethality associated with some aspects of the vascular system (11).

In sharp contrast, results from the present study of LP$_{B3}$-null mice failed to identify functional, anatomical, histological, or hematological defects that might have been expected based on the prior *in vitro* studies or the deletion of LP$_{B1}$. A slight but

statistically significant difference was observed in the average litter size from homozygous intercrosses that produced smaller litters than the crosses between heterozygous males and wild-type females (Table I); the reason for this difference is not known. It was somewhat surprising that a more pronounced defect was not observed in reproductive tissues in view of normally high lp_{B3} expression (Fig. 1) and prior work implicating S1P in testis and oocyte function (33, 34). However, reproductive tissues in LP$_{B3}$-null mice appeared to be histologically and functionally normal. A simple explanation for this phenotype could be compensation by other LP receptors, which necessitated their examination in this study. Both lp_{B1} and lp_{B2} genes were expressed throughout many tissues, similar to lp_{B3} (Fig. 1). Previous receptor overexpression experiments have indicated that LP$_{B2}$ resembles LP$_{B3}$ in coupling to G$_q$, G$_{i/o}$, and G$_{13}$ (35) and mediates S1P-induced PLC activation, adenylyl cyclase activation, cell rounding, proliferation, and suppression of apoptosis (27, 28, 30, 36). Possible compensatory overexpression of lp_{B2} was observed in brain and heart of LP$_{B3}$-null mice (Fig. 3*D*), which might rescue the loss of LP$_{B3}$ functions in those tissues.

The phenotype found in LP$_{B3}$-null mice demonstrates that LP$_{B3}$ is not required for normal organismal development and function and contrasts with the phenotype of LP$_{B1}$-null mice. Deletion of LP$_{B3}$ additionally provided the opportunity to examine its role in S1P signaling using primary cells rather than cell lines; this approach revealed several significant differences compared with prior studies. MEF cells prepared from developing embryos expressed lp_{B1}, lp_{B2}, and lp_{B3} but neither lp_{B4} nor lp_{C1} (Fig. 4) and were highly responsive to S1P in PLC activation, inhibition of cAMP accumulation, and Rho activation (Figs. 5–7). A comparison between the wild-type and knockout MEF cells was used to clarify LP$_{B3}$ involvement in each of the S1P-induced signaling pathways in native cells, which it has not been possible to address previously. No compensatory overexpression of the other S1P genes was observed in the LP$_{B3}$-null MEF cells (Fig. 4), providing the further opportunity to rescue (for LP$_{B3}$) or overexpress various receptors in native cells by retroviral transduction (14), followed by analyses of affected signaling pathways.

Previous overexpression studies have indicated that LP$_{B3}$ mediates S1P-induced PLC activation via both PTX-insensitive and -sensitive pathways (28, 37, 38). The present study indicates that LP$_{B3}$ is predominantly involved in S1P-induced PLC activation through PTX-insensitive G proteins in primary cultures of MEF cells. LP$_{B1}$ appears to mediate a minor component of PLC activation through a G$_{i/o}$ pathway, since the PLC response that remains in the LP$_{B3}$-null MEF cells was fully PTX-sensitive. LP$_{B1}$-overexpressing Chinese hamster ovary cells have been previously shown to induce PTX-sensitive PLC activation (21, 37). Several studies reported that S1P-induced PLC activation occurs through LP$_{B2}$ (37–40) and LP$_{C1}$ (41) but not LP$_{B4}$ (42). None of these receptors could be shown to participate in S1P-induced PLC activation in the present study using MEF cells.

LP$_{B3}$ was also partially involved in the inhibition of adenylyl cyclase activation via a PTX-sensitive G$_{i/o}$-mediated pathway; however, the LP$_{B1}$-mediated pathway appears to be dominant. LP$_{B3}$ has been reported as both an activator (28, 39) and inhibitor (37) of adenylyl cyclase systems. In LP$_{B3}$-null MEF cells, S1P did not increase the basal cAMP levels, whereas infection with LP$_{B3}$-expressing virus could produce S1P-induced increase in basal cAMP levels (~2-fold at 1 μM; data not shown). This suggests that the LP$_{B3}$ receptor can activate adenylyl cyclase when overexpressed but not in native cells. Overexpression of LP$_{B1}$ and LP$_{B4}$ caused adenylyl cyclase in-

hibition, consistent with previous reports (21, 23, 28, 42). A striking result in the analysis of MEF cells was the marked adenylyl cyclase activation by LP$_{C1}$ expression. This receptor has been previously shown to induce intracellular calcium mobilization and activate PLC and mitogen-activated protein kinase, all via PTX-sensitive G$_{i/o}$-mediated pathways (41, 43). The biological significance of this result is unclear, but its occurrence in primary cells suggests that LP$_{C1}$ may function in this manner under some *in vivo* circumstances.

In previous receptor overexpression studies in Chinese hamster ovary cells, Okamoto *et al.* (29) reported that LP$_{B3}$ mediated S1P-induced Rho and Rac activation, whereas LP$_{B1}$ mediated only Rac activation and LP$_{B2}$ mediated only Rho activation. In a similar Chinese hamster ovary system, Paik *et al.* (32) reported that both LP$_{B1}$ and LP$_{B3}$ mediated S1P-induced activation of both Rho and Rac. Analyses of Rho activation in LP$_{B3}$-null MEF cells showed that S1P activated Rho to an extent similar to wild-type cells. Since Rho activation in wild-type cells was PTX-insensitive and LP$_{B1}$ involves PTX-sensitive pathway(s), LP$_{B2}$ appears to be the major receptor for Rho activation in MEF cells. Rac activation, induced by S1P, was also reported in wild-type MEF cells but not in LP$_{B1}$-null MEF cells (11). This contrasts with our results in which we found MEF cells to be highly responsive to S1P in Rho activation but not in Rac activation. The reason for this difference is unclear, but it may reflect variables associated with MEF cell preparations or cell growth conditions.

It is clear from the present study that the deletion of individual LP receptors can produce remarkably different phenotypes as assessed in mice. A previous study on the deletion of LP$_{B1}$ demonstrated embryonic lethality associated with altered S1P signaling properties (Rac activation and chemotaxis) in primary cultures of MEF cells (11). By contrast, no obvious phenotypic abnormalities in the LP$_{B3}$-null mice have been identified, but a strong influence was observed on PLC activation. Our data demonstrate selective attributes for individual S1P receptors in both phenotypic influences and activated signaling pathways. Further studies in which mutant mice are challenged may reveal other roles not apparent in the present studies of the basal state. Viability of these LP$_{B3}$-nulls raises the possibility of future analyses in which more than one LP receptor is genetically deleted.

REFERENCES

1. Hla, T., Lee, M. J., Ancellin, N., Liu, C. H., Thangada, S., Thompson, B. D., and Kluk, M. (1999) *Biochem. Pharmacol.* **58,** 201–207
2. Moolenaar, W. H. (1999) *Exp. Cell Res.* **253,** 230–238
3. Spiegel, S. (1999) *J. Leukocyte Biol.* **65,** 341–344
4. Chun, J., Contos, J. J., and Munroe, D. (1999) *Cell Biochem. Biophys.* **30,** 213–242
5. Pyne, S., and Pyne, N. J. (2000) *Biochem. J.* **349,** 385–402
6. Fukushima, N., Ishii, I., Contos, J. J., Weiner, J. A., and Chun, J. (2001) *Annu. Rev. Pharmacol. Toxicol.* **41,** 507–534
7. Lynch, K. R., and Im, D. S. (1999) *Trends Pharmacol. Sci.* **20,** 473–475
8. Pyne, S., and Pyne, N. (2000) *Pharmacol. Ther.* **88,** 115–131
9. Zhang, G., Contos, J. J., Weiner, J. A., Fukushima, N., and Chun, J. (1999) *Gene (Amst.)* **227,** 89–99
10. Contos, J. J., Ishii, I., and Chun, J. (2000) *Mol. Pharmacol.* **58,** 1188–1196
11. Liu, Y., Wada, R., Yamashita, T., Mi, Y., Deng, C. X., Hobson, J. P., Rosenfeldt, H. M., Nava, V. E., Chae, S. S., Lee, M. J., Liu, C. H., Hla, T., Spiegel, S., and Proia, R. L. (2000) *J. Clin. Invest.* **106,** 951–961
12. Kupperman, E., An, S., Osborne, N., Waldron, S., and Stainier, D. Y. (2000) *Nature* **406,** 192–195
13. Marth, J. D. (1996) *J. Clin. Invest.* **97,** 1999–2002
14. Ishii, I., Contos, J. J., Fukushima, N., and Chun, J. (2000) *Mol. Pharmacol.* **58,** 895–902
15. Weiner, J. A., Hecht, J. H., and Chun, J. (1998) *J. Comp. Neurol.* **398,** 587–598
16. Chun, J. J., Schatz, D. G., Oettinger, M. A., Jaenisch, R., and Baltimore, D. (1991) *Cell* **64,** 189–200
17. Ishii, I., Izumi, T., Tsukamoto, H., Umeyama, H., Ui, M., and Shimizu, T. (1997) *J. Biol. Chem.* **272,** 7846–7854
18. An, S., Bleu, T., Zheng, Y., and Goetzl, E. J. (1998) *Mol. Pharmacol.* **54,** 881–888
19. Kimura, Y., Schmitt, A., Fukushima, N., Ishii, I., Kimura, H., Nebreda, A. R., and Chun, J. (2001) *J. Biol. Chem.* **276,** 15208–15215
20. An, S., Bleu, T., Huang, W., Hallmark, O. G., Coughlin, S. R., and Goetzl, E. J. (1997) *FEBS Lett.* **417,** 279–282
21. Okamoto, H., Takuwa, N., Gonda, K., Okazaki, H., Chang, K., Yatomi, Y., Shigematsu, H., and Takuwa, Y. (1998) *J. Biol. Chem.* **273,** 27104–27110
22. Lee, M. J., Van Brocklyn, J. R., Thangada, S., Liu, C. H., Hand, A. R., Menzeleev, R., Spiegel, S., and Hla, T. (1998) *Science* **279,** 1552–1555
23. Zondag, G. C., Postma, F. R., Etten, I. V., Verlaan, I., and Moolenaar, W. H. (1998) *Biochem. J.* **330,** 605–609
24. Im, D. S., Heise, C. E., Ancellin, N., O'Dowd, B. F., Shei, G. J., Heavens, R. P., Rigby, M. R., Hla, T., Mandala, S., McAllister, G., George, S. R., and Lynch, K. R. (2000) *J. Biol. Chem.* **275,** 14281–14286
25. Contos, J. J., Fukushima, N., Weiner, J. A., Kaushal, D., and Chun, J. (2000) *Proc. Natl. Acad. Sci. U. S. A.* **97,** 13384–13389
26. Kimura, T., Watanabe, T., Sato, K., Kon, J., Tomura, H., Tamama, K., Kuwabara, A., Kanda, T., Kobayashi, I., Ohta, H., Ui, M., and Okajima, F. (2000) *Biochem. J.* **348,** 71–76
27. An, S., Zheng, Y., and Bleu, T. (2000) *J. Biol. Chem.* **275,** 288–296
28. Kon, J., Sato, K., Watanabe, T., Tomura, H., Kuwabara, A., Kimura, T., Tamama, K., Ishizuka, T., Murata, N., Kanda, T., Kobayashi, I., Ohta, H., Ui, M., and Okajima, F. (1999) *J. Biol. Chem.* **274,** 23940–23947
29. Okamoto, H., Takuwa, N., Yokomizo, T., Sugimoto, N., Sakurada, S., Shigematsu, H., and Takuwa, Y. (2000) *Mol. Cell. Biol.* **20,** 9247–9261
30. Van Brocklyn, J. R., Tu, Z., Edsall, L. C., Schmidt, R. R., and Spiegel, S. (1999) *J. Biol. Chem.* **274,** 4626–4632
31. Lee, M. J., Thangada, S., Claffey, K. P., Ancellin, N., Liu, C. H., Kluk, M., Volpi, M., Sha'afi, R. I., and Hla, T. (1999) *Cell* **99,** 301–312
32. Paik, J. H., Chae, S., Lee, M. J., Thangada, S., and Hla, T. (2001) *J. Biol. Chem.* **276,** 11830–11837
33. Yatomi, Y., Igarashi, Y., Yang, L., Hisano, N., Qi, R., Asazuma, N., Satoh, K., Ozaki, Y., and Kume, S. (1997) *J. Biochem. (Tokyo)* **121,** 969–973
34. Morita, Y., Perez, G. I., Paris, F., Miranda, S. R., Ehleiter, D., Haimovitz-Friedman, A., Fuks, Z., Xie, Z., Reed, J. C., Schuchman, E. H., Kolesnick, R. N., and Tilly, J. L. (2000) *Nat. Med.* **6,** 1109–1114
35. Windh, R. T., Lee, M. J., Hla, T., An, S., Barr, A. J., and Manning, D. R. (1999) *J. Biol. Chem.* **274,** 27351–27358
36. Ancellin, N., and Hla, T. (1999) *J. Biol. Chem.* **274,** 18997–9002
37. Okamoto, H., Takuwa, N., Yatomi, Y., Gonda, K., Shigematsu, H., and Takuwa, Y. (1999) *Biochem. Biophys. Res. Commun.* **260,** 203–208
38. An, S., Bleu, T., and Zheng, Y. (1999) *Mol. Pharmacol.* **55,** 787–794
39. Gonda, K., Okamoto, H., Takuwa, N., Yatomi, Y., Okazaki, H., Sakurai, T., Kimura, S., Sillard, R., Harii, K., and Takuwa, Y. (1999) *Biochem. J.* **337,** 67–75
40. Tamama, K., Kon, J., Sato, K., Tomura, H., Kuwabara, A., Kimura, T., Kanda, T., Ohta, H., Ui, M., Kobayashi, I., and Okajima, F. (2001) *Biochem. J.* **353,** 139–146
41. Yamazaki, Y., Kon, J., Sato, K., Tomura, H., Sato, M., Yoneya, T., Okazaki, H., Okajima, F., and Ohta, H. (2000) *Biochem. Biophys. Res. Commun.* **268,** 583–589
42. Malek, R. L., Toman, R. E., Edsall, L. C., Wong, S., Chiu, J., Letterle, C. A., Van Brocklyn, J. R., Milstien, S., Spiegel, S., and Lee, N. H. (2001) *J. Biol. Chem.* **276,** 5692–5699
43. Van Brocklyn, J. R., Graler, M. H., Bernhardt, G., Hobson, J. P., Lipp, M., and Spiegel, S. (2000) *Blood* **95,** 2624–2629